

Spin Sum Rules and the Strong Coupling Constant at large distance.

A. Deur

Thomas Jefferson National Accelerator Facility, Newport News, VA 23606

Abstract. We present recent results on the Bjorken and the generalized forward spin polarizability sum rules from Jefferson Lab Hall A and CLAS experiments, focusing on the low Q^2 part of the measurements. We then discuss the comparison of these results with Chiral Perturbation theory calculations. In the second part of this paper, we show how the Bjorken sum rule with its connection to the Gerasimov-Drell-Hearn sum, allows us to conveniently define an effective coupling for the strong force at all distances.

Keywords: Strong coupling constant, QCD spin sum rules, non-perturbative, commensurate scale relations, Schwinger-Dyson, Lattice QCD, AdS/CFT

PACS: 12.38Qk, 11.55Hx

INTRODUCTION

The information on the longitudinal spin structure of the nucleon is contained in the $g_1(x, Q^2)$ and $g_2(x, Q^2)$ spin structure functions, with Q^2 the squared four-momentum transferred from the beam to the target, and $x = Q^2/(2M\nu)$ the Bjorken scaling variable (ν is the energy transfer and M the nucleon mass). The variable Q^2 indicates the space-time scale at which the nucleon is probed and x is interpreted in the parton model as the fraction of nucleon momentum carried by the struck quark.

Although spin structure functions are the basic observables for nucleon spin studies, considering their integrals taken over x is advantageous because of resulting simplifications. More importantly, such integrals are at the core of the relation dispersion formalism. Relation dispersions relate the integral over the imaginary part of a quantity to its real part. Expressing the imaginary part in function of the real part using the optical theorem yields *sum rules*. When additional hypotheses are used, such as a low energy theorem or the validity of Operator Product Expansion (OPE), the sum rules relate the integral to a static property of the target. If the static property is well known, the verification of the sum rule provides a check of the theory and hypotheses used in the sum rule derivation. When the property is not known because e.g. it is difficult to measure directly, sum rules can be used to access them. In that case, the theoretical framework used to derived the sum rule is assumed to be valid. Details on integrals of spin structure functions and sum rules are given e.g. in the review [1].

Several spin sum rules exists. We will focus on the Bjorken sum rule [2] and spin polarizability sum rules. We will only briefly discuss the Gerasimov-Drell-Hearn (GDH) sum rule [3] since it is covered by V. Sulkosky's talk at this conference. In this paper, we will consider the n -th Cornwall-Norton moments: $\int_0^1 dx g_1^N(x, Q^2) x^n$, with N standing for proton or neutron, and write the first moments as $\Gamma_1^N(Q^2) \equiv \int_0^1 dx g_1^N(x, Q^2)$.

THE GENERALIZED BJORKEN AND GDH SUM RULES

The Bjorken sum rule [2] relates the integral over $(g_1^p - g_1^n)$ to the nucleon axial charge g_A . This relation has been essential for understanding the nucleon spin structure and establishing, *via* its Q^2 -dependence, that Quantum Chromodynamics (QCD) describes the strong force when spin is included. The Bjorken integral has been measured in polarized deep inelastic lepton scattering (DIS) at SLAC, CERN and DESY [6]-[9] and at moderate Q^2 at Jefferson Lab (JLab) [17]-[19]. In the perturbative QCD (pQCD) domain (high Q^2) the sum rule reads:

$$\Gamma_1^{p-n}(Q^2) \equiv \int_0^1 dx (g_1^p(x, Q^2) - g_1^n(x, Q^2)) = \frac{g_A}{6} \left[1 - \frac{\alpha_s}{\pi} - 3.58 \frac{\alpha_s^2}{\pi^2} - 20.21 \frac{\alpha_s^3}{\pi^3} + \dots \right] + \sum_{i=2}^{\infty} \frac{\mu_{2i}^{p-n}(Q^2)}{Q^{2i-2}} \quad (1)$$

where $\alpha_s(Q^2)$ is the strong coupling strength. The bracket term (known as the leading twist term) is mildly dependent on Q^2 due to pQCD soft gluon radiation. The other term contains non-perturbative power corrections (higher twists). These are quark and gluon correlations describing the nucleon structure away from the large Q^2 (small distances) limit.

The generalized Bjorken sum rule has been derived for small distances. For large distances, in the $Q^2 \rightarrow 0$ limit, one finds the generalized GDH sum rule. The sum rule was first derived at $Q^2 = 0$:

$$\int_{v_0}^{\infty} \frac{\sigma_{1/2}(v) - \sigma_{3/2}(v)}{v} dv = -\frac{2\pi^2 \alpha \kappa^2}{M_t^2} \quad (2)$$

where v_0 is the pion photoproduction threshold, $\sigma_{1/2}$ and $\sigma_{3/2}$ are the helicity dependent photoproduction cross sections for total photon plus target helicities 1/2 and 3/2, κ is the anomalous magnetic moment of the target while S is its spin and M_t its mass. α is the fine structure constant.

Replacing the photoproduction cross sections by the electroproduction ones generalized the left hand side of Eq. 2 to any Q^2 . Such generalization depends on the choice of convention for the virtual photon flux, see e.g. ref. [1]. X. Ji and J. Osborne [20] showed that the sum *rule* itself (i.e. the whole Eq. 2) can be generalized as:

$$\frac{8}{Q^2} \int_0^{x^-} g_1 dx = s_1(0, Q^2) \quad (3)$$

where $S_1(v, Q^2)$ is the spin dependent Compton amplitude. This generalization of the GDH sum rule makes the connection between the Bjorken and GDH generalized sum rules evident: $\text{GDH} = \frac{Q^2}{8} \times \text{Bjorken}$.

The connection between the GDH and Bjorken sum rules allows us in principle to compute the moment Γ_1 at any Q^2 . Thus, it provides us with a choice observable to understand the transition of the strong force from small to large distances.

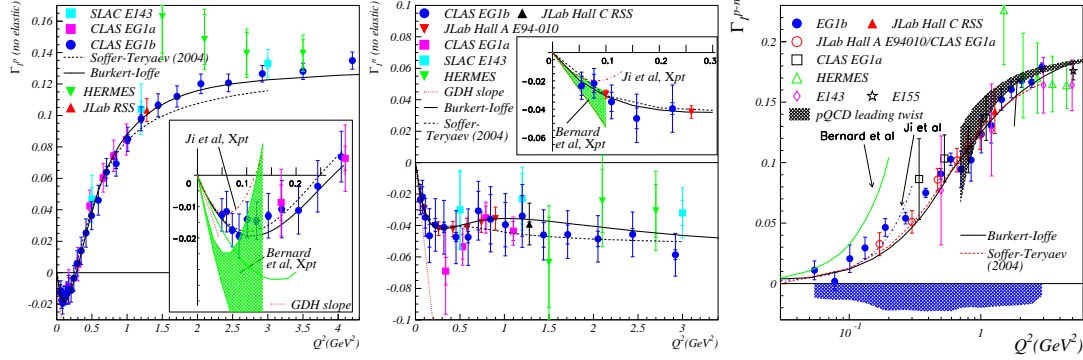


FIGURE 1. (Color online) Experimental data from SLAC, CERN, DESY and JLab at low and intermediate Q^2 on Γ_1^p (left), Γ_1^n (center) and Γ_1^{p-n} (right).

EXPERIMENTAL MEASUREMENTS OF THE FIRST MOMENTS

Results from experimental measurements from SLAC [6], CERN [8], DESY [9] and JLab [10]-[19] of the first moments are shown in Figure 1. There is an excellent mapping of the moments at intermediate Q^2 and enough data points a low Q^2 to start testing the Chiral Perturbation Theory (χPT), the effective theory strong force at large distances. In particular, the Bjorken sum is important for such test because the (p-n) subtraction cancels the Δ_{1232} resonance contribution which should make the χPT calculations significantly more reliable [21]. The comparison between the data at low Q^2 and χPT calculations [22],[23] can be seen more easily in the insert in each plot of Fig. 1. The calculations assume the Γ_1 slope at $Q^2=0$ from the GDH sum rule prediction. Consequently, χPT calculates the deviation from the slope and this is what one should test. A meaningful comparison is provided by fitting the lowest data points using the form $\Gamma_1^N = \frac{\kappa_N^2}{8M^2} Q^2 + aQ^4 + bQ^6 \dots$ and compare the obtained value of a to the values calculated from χPT . Such comparison has been carried out for the proton, deuteron [16] and the Bjorken sum [18] (the results are given in Fig. 3). These fits point out the importance of including a Q^6 term for $Q^2 < 0.1 \text{ GeV}^2$. The χPT calculations seems to agree best with the measurement of the Bjorken sum, in accordance with the discussion in [21]. Phenomenological models [24],[25] are in good agreement with the data over the whole Q^2 range.

SPIN POLARIZABILITY SUM RULES

Higher moments of g_1 and g_2 are connected by sum rules to spin polarizabilities. Those characterize the coherent response of the nucleon to photons. They are defined using low-energy theorems in the form of a series expansion in the photon energy. The first term of the series comes from the spatial distribution of charge and current (form factors) while the second term results from the deformation of these distributions induced by the photon (polarizabilities). Hence, polarizabilities are as important as form factors in

understanding coherent nucleon structure. *Generalized* spin polarizabilities describe the response to *virtual* photons. The low energy theorem defining the generalized forward spin polarizability γ_0 is:

$$\Re[g_{TT}(v, Q^2) - g_{TT}^{pole}(v, Q^2)] = \left(\frac{2\alpha}{M^2}\right)I_{TT}(Q^2)v + \gamma_0(Q^2)v^3 + O(v^5), \quad (4)$$

where g_{TT} is the spin-flip doubly-virtual Compton scattering amplitude, and I_{TT} is the coefficient of the $O(v)$ term of the Compton amplitude which can be used to generalize the GDH sum rule to non-zero Q^2 . We have $I_{TT}(Q^2 = 0) = \kappa/4$. In practice γ_0 can be obtained from a sum rule which has a derivation akin to that of the GDH sum rule:

$$\gamma_0 = \frac{16\alpha M^2}{Q^6} \int_0^{x_0} x^2 \left(g_1 - \frac{4M^2}{Q^2} x^2 g_2 \right) dx, \quad (5)$$

Similar relations define the generalized longitudinal-transverse polarizability δ_{LT} :

$$\Re[g_{LT}(v, Q^2) - g_{LT}^{pole}(v, Q^2)] = \left(\frac{2\alpha}{M^2}\right)QI_{LT}(Q^2) + Q\delta_{LT}(Q^2)v^2 + O(v^4), \quad (6)$$

$$\delta_{LT} = \frac{16\alpha M^2}{Q^6} \int_0^{x_0} x^2 (g_1 + g_2) dx. \quad (7)$$

where g_{LT} is the longitudinal-transverse interference amplitude, and I_{LT} is the coefficient of the $O(v)$ term of the Compton amplitude. Details on the derivation of Eqs. 4-7 can be found in [1]. Higher moments are advantageous because they are essentially free of the uncertainty associated with the low- x extrapolation necessary since reaching $x \rightarrow 0$ would require an infinite beam energy. Eqs. 5 and 7 are examples of uses of sum rules to measure observables that are otherwise hard to access.

In the case of the transverse-longitudinal polarizability δ_{LT} , the Δ_{1232} contribution is suppressed at low Q^2 because the N- Δ transition is mostly transverse, making the contribution of the Δ to the longitudinal-transverse (LT) interference term very small. Thus δ_{LT} should also provide a reliable test of χPT computations. Furthermore, as for the Bjorken sum the isovector part of γ_0 , $\gamma_0^p - \gamma_0^n$, should offers similar advantages for checking the calculation techniques of χPT . The low Q^2 data on forward spin polarizabilities, from Hall A E94010 and CLAS EG1b, are shown on Fig. 2 There is no agreement between the data and the χPT calculations (except possibly for the lowest Q^2 point of γ_0^n that agrees with the explicitly covariant calculation of Bernard *et al*). Such disagreement is surprising because the first point should be into the validity domains of χPT . It is even more surprising for δ_{LT}^n and γ_0^{p-n} because of the Δ suppression for these two quantities. This points out that including the Δ in the calculations may not be the only challenge facing χPT theorists. In contrast, the MAID model [26] is in good agreement with the data. Figure 3 summarizes the comparison between χPT calculations and data. (We added the higher moment d_2^n measured in Experiment E94010).

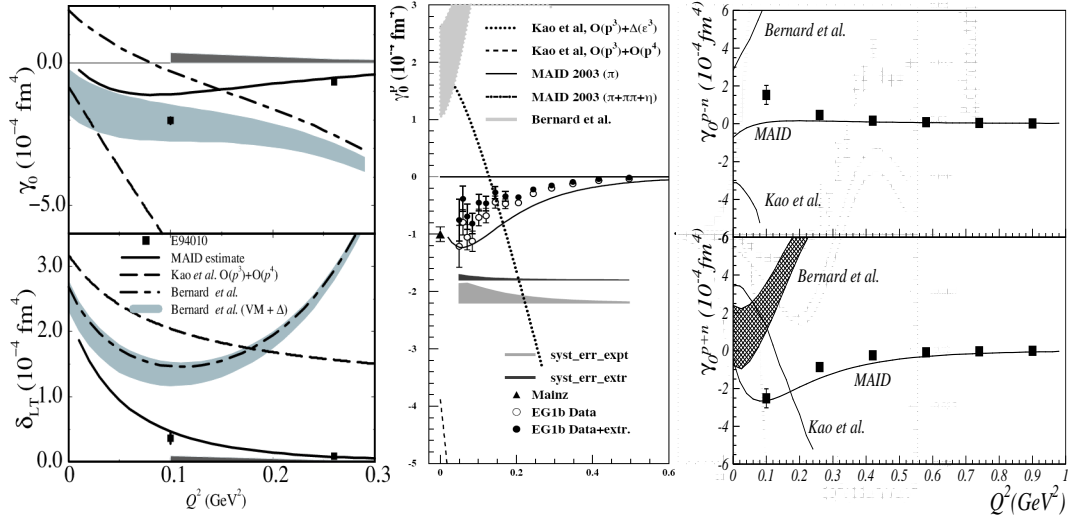


FIGURE 2. Experimental data at low Q^2 on generalized spin polarizabilities. Results on neutron (JLab Hall A experiment E94010 [14]) are shown on the left (top: γ_0^n , bottom: δ_{LT}^n). Results on the proton (JLab CLAS experiment EG1b [16]) γ_0^p are shown in the central plot. The isospin decomposition of γ_0 (E94010+EG1b [18]) is shown on the right (top: γ_0^{p-n} , bottom γ_0^{p+n}).

		No low-x ↓	No low-x No Δ ↓	No low-x ↓
	Γ_1	γ_0	δ_{LT}	d_2
	Proton	$a^{\text{exp}}=4.31\pm0.31\pm1.36$ $a^h=3.89$ Up to $Q^2\sim0.08 \text{ GeV}^2$		No low Q^2 data
	Neutron		Up to $Q^2\sim0.1 \text{ GeV}^2$ (Bernard <i>et al.</i> only)	
No Δ →	P-N	$a^{\text{exp}}=0.80\pm0.07\pm0.23$ $a^h=0.74, a^h=2.4$ Up to $Q^2\sim0.3 \text{ GeV}^2$		No low Q^2 data
	P+N	$a^{\text{exp}}=6.97\pm0.96\pm1.48$ $a^h=7.11$ Up to $Q^2\sim0.1 \text{ GeV}^2$		No low Q^2 data

FIGURE 3. (Color online) Summary the comparison between χPT calculations and data. The green indicates a good match within the region in which we expect the chiral perturbation series to be reliable, the yellow an agreement over a shorter Q^2 range, and the red a mismatch.

THE STRONG COUPLING AT LARGE DISTANCES

So far, we have discussed the data at low Q^2 . The primary goal of the JLab experiments was to map precisely the intermediate Q^2 range in order to shed light on the transition from short distances (where the degrees of freedom pertinent to the strong force are the partonic ones) to large distances where the hadronic degrees of freedom are relevant to

the strong force. One feature seen on Fig. 1 is that the transition from small to large distances is smooth, e.g. without sign of a phase transition. This fact can be used to extrapolate the definition of the strong force effective coupling to large distances. Before discussing this, we first review the QCD coupling and the issues with calculating it at large distances.

In QCD, the magnitude of the strong force is given by the running coupling constant α_s . At large Q^2 , in the pQCD domain, α_s is well defined and is given by the series:

$$\mu \frac{\partial \alpha_s}{\partial \mu} = 2\beta(\alpha_s) = -\frac{\beta_0}{2\pi}\alpha_s^2 - \frac{\beta_1}{4\pi^2}\alpha_s^3 - \frac{\beta_2}{64\pi^3}\alpha_s^4 - \dots \quad (8)$$

Where μ is the energy scale, to be identified to Q . The first terms of the β series are: $\beta_0 = 11 - \frac{2}{3}n$ with n the number of active quark flavors, $\beta_1 = 51 - \frac{19}{3}n$ and $\beta_2 = 2857 - \frac{5033}{9}n + \frac{325}{27}n^2$. The solution of the differential equation 8 is:

$$\alpha_s(\mu) = \frac{4\pi}{\beta_0 \ln(\mu^2/\Lambda_{QCD}^2)} \times \left[1 - \frac{2\beta_1}{\beta_0^2} \frac{\ln[\ln(\mu^2/\Lambda_{QCD}^2)]}{\ln(\mu^2/\Lambda_{QCD}^2)} + \frac{4\beta_1^2}{\beta_0^4 \ln^2(\mu^2/\Lambda_{QCD}^2)} \left(\left(\ln[\ln(\mu^2/\Lambda_{QCD}^2)] - \frac{1}{2} \right)^2 + \frac{\beta_2\beta_0}{8\beta_1^2} - \frac{5}{4} \right) \right] \quad (9)$$

Equation 9 allows us to evolve the different experimental determinations of α_s to a conventional scale, typically $M_{z_0}^2$. The agreement between the α_s obtained from different observables demonstrates its universality and the validity of Eq. 8. One can obtain $\alpha_s(M_{z_0}^2)$ with doubly polarized DIS data and assuming the validity of the Bjorken sum. Solving Eq. 1 using the experimental value of Γ_1^{p-n} , and then using Eq. 9 provides $\alpha_s(M_{z_0}^2)$.

Equation 9 leads to an infinite coupling at large distances, when Q^2 approaches Λ_{QCD}^2 . This is not a conceptual problem since we are out of the validity domain of pQCD on which Eq. 9 is based. But since data show no sign of discontinuity or phase transition when crossing the intermediate Q^2 domain, one should be able to define an effective coupling α_s^{eff} at any Q^2 that matches α_s at large Q^2 but stays finite at small Q^2 .

The Bjorken Sum Rule can be used to define α_s^{eff} at low Q^2 . Defining α_s^{eff} from a pQCD equation truncated to first order (in our case Eq. (1: $\Gamma_1^{p-n} \equiv \frac{1}{6}(1 - \alpha_{s,g1}/\pi)$), offers advantages. In particular, α_s^{eff} does not diverge near Λ_{QCD} and is renormalization scheme independent. However, α_s^{eff} becomes dependent on the choice of observable employed to define it. If Γ_1^{p-n} is used as the defining observable, the effective coupling is noted $\alpha_{s,g1}$. Relations, called *commensurate scale relations* [27], link the different effective couplings so in principle one effective coupling is enough to describe the strong force and the theory retains its predictive power. These relations are defined for short distances and whether they extrapolate to large distances remains to be investigated.

The choice of defining the effective charge with the Bjorken sum has many advantages: low Q^2 data exist and near real photons data from JLab is being analyzed [28, 29]. Furthermore, sum rules constrain $\alpha_{s,g1}$ at both low and large Q^2 , as will be discussed in the next paragraph. Another advantage is that, as discussed for the low Q^2 domain,

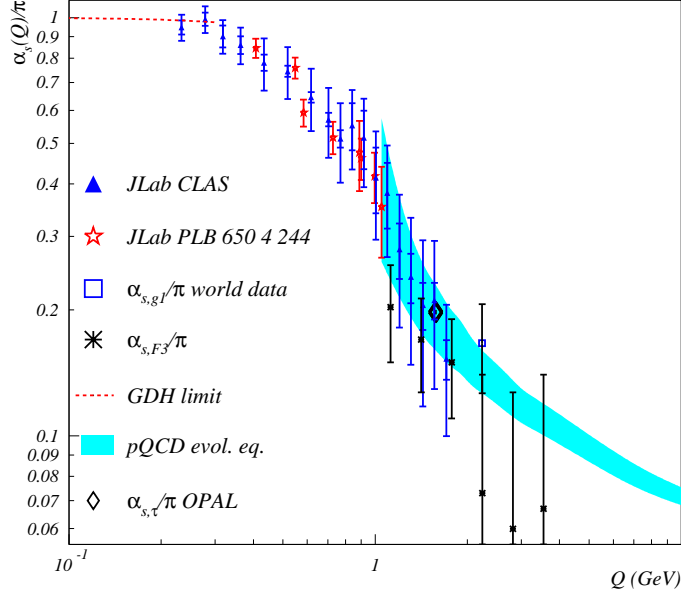


FIGURE 4. Value of $\alpha_{s,g1}/\pi$ extracted from the world data on the Bjorken sum at $Q^2 = 5 \text{ GeV}^2$ [7] and from JLab data [10, 18]. Also shown are $\alpha_{s,\tau}$ extracted from the OPAL data on τ decay [27], and $\alpha_{s,GLS}$ extracted using the Gross-Llewellyn Smith sum rule [32] and its measurement by the CCFR collaboration [33]. The gray band indicates $\alpha_{s,g1}$ extracted from the pQCD expression of the Bjorken sum at leading twist and third order in α_s (with α_s computed using Eq. 9). The values of $\alpha_{s,g1}/\pi$ extracted using the Gerasimov-Drell-Hearn sum rule is given by the red dashed line.

the simplification arising in Γ_1^{p-n} makes a quantity well suited to be calculated at any Q^2 [21]. These simplifications are manifest at large Q^2 when comparing the validities of the Bjorken and Ellis-Jaffe sum rules. It also simplifies Lattice QCD calculations in the intermediate Q^2 domain. Finally, it may be argued that $\alpha_{s,g1}$ might be more directly comparable to theoretical calculations than other effective couplings extracted from other observables: part of the coherent response of the nucleon is suppressed in the Bjorken sum, e.g. the Δ resonance, so the non-resonant background, akin to the pQCD incoherent scattering process, contributes especially importantly to the Bjorken sum. This argument is reinforced if global duality works, a credible proposal since the Δ resonance is suppressed.

The effective coupling definition in terms of pQCD evolution equations truncated to first order was proposed by Grunberg [30]. Grunberg's definition is meant for short distances but one can always extrapolated this definition and see how the resulting coupling compares to calculation of α_s at large distances. Using Grunberg's definition at large distances entails including higher twists in $\alpha_{s,g1}$ in addition to the higher terms of the pQCD series. Effective couplings have been extracted from different observables and have been compared to each other using the commensurate scale relations [31], see Fig. 4. There is good agreement between $\alpha_{s,g1}$, $\alpha_{s,F3}$ and $\alpha_{s,\tau}$. The GDH and Bjorken sum rules can be used to extract $\alpha_{s,g1}$ at small and large Q^2 respectively [31]. This, together

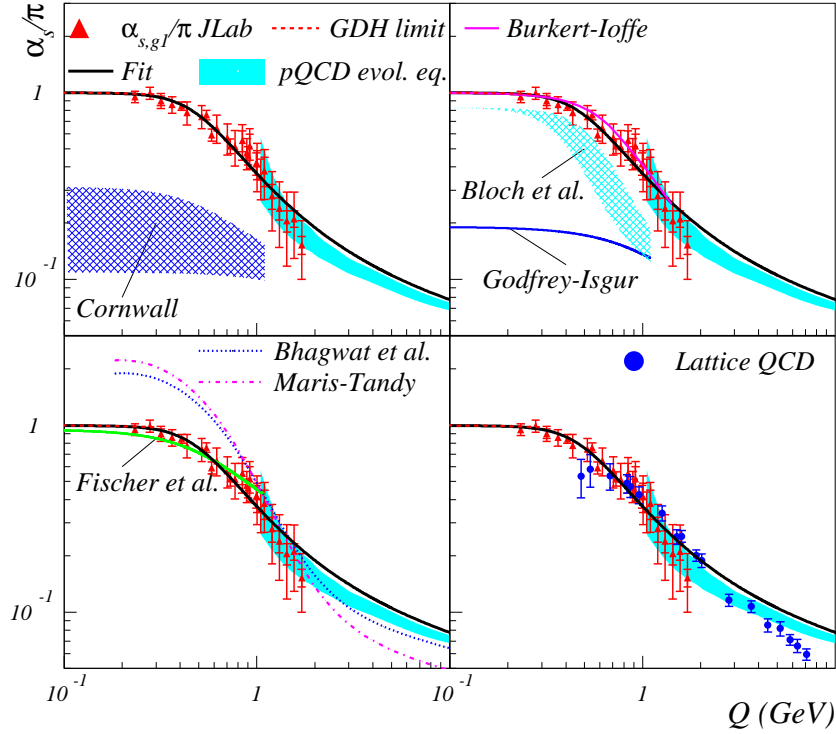


FIGURE 5. The effective coupling α_{s,g_1} extracted from JLab data, its fit, and its extraction using the Burkert and Ioffe [24] model to obtain Γ_1^{p-n} . The α_s calculations are: Top left: Schwinger-Dyson equations (Cornwall [35]); Top right: Schwinger-Dyson equations (Bloch) [36] and α_s used in a quark constituent model [37]; Bottom left: Schwinger-Dyson equations (Maris-Tandy [38]), Fischer, Alkofer, Reinhardt and Von Smekal [39] and Bhagwat et al. [40]; Bottom right: Lattice QCD [41].

with the JLab data at intermediate Q^2 , provides for the first time a coupling at any Q^2 . A striking feature of Fig. 4 is that α_{s,g_1} becomes scale invariant at small Q^2 . This was predicted by a number of calculations and it is known that color confinement leads to an infrared fixed point [34], but it is the first time it is seen experimentally. A fit of the α_{s,g_1} has been performed and is shown on Fig. 5 (plain black line).

In Figure 5, α_{s,g_1} is compared to theoretical results. There are several techniques used to predict α_s at small Q^2 , e.g. lattice QCD, solving the Schwinger-Dyson equations, or choosing the coupling in a constituent quark model so that it reproduces hadron spectroscopy. However, the connection between these α_s is unclear, in part because of the different approximations used. In addition, the precise relation between α_{s,g_1} (or any effective coupling defined using [30] or [27]) and these computations is unknown. Nevertheless, one can still compare them to see if they share common features. The calculations and α_{s,g_1} present a similar behavior. Some calculations, in particular the lattice one, are in excellent agreement with α_{s,g_1} .

These works show that α_s is scale invariant (*conformal behavior*) at small and large

Q^2 (but not in the transition region between the fundamental description of QCD in terms of quarks and gluons degrees of freedom and its effective one in terms of baryons and mesons). The scale invariance at large Q^2 is the well known asymptotic freedom. The conformal behavior at small Q^2 is essential to apply a property of *conformal field theories* (CFT) to the study of hadrons: the *Anti-de-Sitter space/Conformal Field Theory* (AdS/CFT) *correspondence* of Maldacena [42], that links a strongly coupled gauge field to weakly coupled superstrings states. Perturbative calculations are feasible in the weak coupling AdS theory. They are then projected on the AdS boundary, where they correspond to the calculations that would have been obtained with the strongly coupled CFT. This opens the possibility of analytic non-perturbative QCD calculations [43].

SUMMARY AND PERSPECTIVES

We discussed the data on moments of spin structure functions at large distances and compared them to χPT , the strong force effective theory at large distances. The data and calculations do not consistently agree. In particular, the better agreement expected for observables in which the Δ resonance is suppressed is seen only for the Bjorken sum, but not for δ_{LT}^n or $\gamma_0^p - \gamma_0^n$. Apparently, the Δ cannot explain single-handedly the discrepancy between data and calculations. The data shown were taken at JLab during experiments focusing on covering the intermediate Q^2 range [10, 18]. A new generation of experiments [28, 29] especially dedicated to push such measurements to lower Q^2 and higher precision has taken new data that are being analyzed. In addition, a new experiment to measure δ_{LT}^p in Hall A at low Q^2 is approved [44], while the frozen spin HD target recently arrived at JLab from BNL is opening new possibilities of measurements with CLAS using transversely polarized protons or deuterons.

The smoothness of Q^2 -dependence of the moments when transiting from perturbative to the non-perturbative domain allows to extrapolate the definitions of effective strong couplings from short to large distances. Thanks to the data on nucleon spin structure and to spin sum rules, the effective strong coupling α_{s,g_1} can be extracted in any regime of QCD. The question of comparing it with theoretical calculations of α_s at low Q^2 is open, but such comparison exposes a similarity between these couplings. Apart for the parton-hadron transition region, the coupling shows that QCD is approximately a conformal theory. This is a necessary ingredient to the application of the AdS/CFT correspondence that may make analytical calculations possible in the non-perturbative domain of QCD.

ACKNOWLEDGMENTS

This work is supported by the U.S. Department of Energy (DOE). The Jefferson Science Associates (JSA) operates the Thomas Jefferson National Accelerator Facility for the DOE under contract DE-AC05-84ER40150.

REFERENCES

1. J.-P. Chen, A. Deur, Z.-E. Meziani; Mod. Phys. Lett. **A 20**, 2745 (2005).

2. J. D. Bjorken, Phys. Rev. **148**, 1467 (1966); **D 1**, 465 (1970); Phys. Rev. D **1**, 1376 (1970).
3. S. D. Drell and A. C. Hearn, Phys. Rev. Lett. **16**, 908 (1966). S. Gerasimov, Sov. J. Nucl. Phys. **2**, 430 (1966).
4. E142 Collaboration, P. L. Anthony *et al.*, Phys. Rev. Lett. **71**, 959 (1993)
5. K. Abe *et al.*, Phys. Rev. Lett. **74**, 346 (1995); **75**, 25 (1995); **76**, 587 (1996); Phys. Lett. **B 364**, 61 (1995); Phys. Rev. **D 58**, 112003 (1998).
6. E154 collaboration: K. Abe *et al.*, Phys. Rev. Lett. **79**, 26 (1997).
7. P. L. Anthony, *et al.*, Phys. Lett. **B 458**, 529 (1999); **B 463**, 339 (1999); **B 493**, 19 (2000); **B 553**, 18 (2003).
8. SMC collaboration: D. Adeva *et al.*, Phys. Rev. D **58**, 112001 (1998).
9. HERMES collaboration: K. Ackerstaff, *et al.*, Phys. Lett. **B 404**, 383 (1997); **B 444**, 531 (1998); A. Airapetian, *et al.*, Phys. Lett. **B 442**, 484 (1998); Phys. Rev. Lett. **90**, 092002 (2003); Eur. Phys. J. C **26**, 527 (2003); Phys. Rev. **D 75**, 012007 (2007).
10. CLAS collaboration: R. Fatemi *et al.*, Phys. Rev. Lett. **91**, 222002 (2003).
11. CLAS collaboration: J. Yun *et al.*, Phys. Rev. C **67**, 055204 (2003).
12. E94-010 collaboration: M. Amarian *et al.*, Phys. Rev. Lett. **89**, 242301 (2002).
13. E94-010 collaboration: M. Amarian *et al.*, Phys. Rev. Lett. **92**, 022301 (2004).
14. E94-010 collaboration: M. Amarian *et al.*, Phys. Rev. Lett. **93**, 152301 (2004).
15. V. Dharmawardane *et al.*, Phys. Lett. **B 641**, 11 (2006).
16. Y. Prok *et al.*, Phys. Lett. **B 672** 12 (2009)
17. A. Deur *et al.*, Phys. Rev. Lett. **93**, 212001-1 (2004).
18. A. Deur *et al.*, Phys. Rev. **D 78** 032001 (2008)
19. K. Slifer, arXiv:0812.0031 (2009)
20. X. Ji et J Osborne, J. of Phys. G **27**, 127 (2001).
21. V. D. Burkert, Phys. Rev. **D 63**, 097904 (2001).
22. V. Bernard, T. R. Hemmert and Ulf-G. Meissner, Phys. Rev. **D 67**, 076008 (2003).
23. X. Ji, C. W. Kao and J. Osborne, Phys. Lett. **B 472**, 1 (2000).
24. V. D. Burkert and B. L. Ioffe, Phys. Lett. **B 296**, 223 (1992); J. Exp. Theor. Phys. **78**, 619 (1994).
25. J. Soffer and O. V. Teryaev, Phys. Lett. **B 545**, 323 (2002); Phys. Rev. **D 70** 116004 (2004).
26. D. Drechsel, S. Kamalov and L. Tiator. Nucl. Phys. A **645**, 145 (1999).
27. S. J. Brodsky and H. J. Lu, Phys. Rev. **D 51**, 3652 (1995); S. J. Brodsky, G. T. Gabadadze, A. L. Kataev and H. J. Lu, Phys. Lett. **B372**, 133 (1996); See also S. J. Brodsky, hep-ph/0310289, S. J. Brodsky, S. Menke, C. Merino and J. Rathsmann, Phys Rev **D67**, 055008 (2003)
28. J.P. Chen, A. Deur and F. Garibaldi, JLab experiment E97-110
29. M. Battaglieri, A. Deur, R. De Vita and M. Ripani, JLab experiment E03-006
30. G. Grunberg, Phys. Lett. **B 95**, 70 (1980); Phys. Rev. **D 29**, 2315 (1984); Phys. Rev. **D 40**, 680 (1989)
31. A. Deur, V. Burkert, J.-P. Chen, W. Korsch, Phys. Lett. **B 650**, 4 244 (2007); A. Deur, V. Burkert, J.-P. Chen, W. Korsch, Phys. Lett. **B665**, 349 (2008)
32. D. J. Gross and C. H. Llewellyn Smith, Nucl. Phys **B14**, 337 (1969)
33. J. H. Kim *et al.*, Phys. Rev. Lett. **81**, 3595 (1998)
34. S. J. Brodsky, R. Shrock, Phys. Lett. **B666** 95 (2008); S. J. Brodsky, G. de Teramond, R. Shrock, arXiv:0807.2484
35. J. M. Cornwall, Phys. Rev. **D26**, 1453 (1982)
36. J. C. R. Bloch, Phys. Rev. **D66**, 034032 (2002)
37. S. Godfrey and N. Isgur, Phys. Rev. **D32**, 189 (1985)
38. P. Maris and P. C. Tandy, Phys. Rev. **C60**, 055214 (1999)
39. C.S. Fischer, R. Alkofer, Phys. Lett. **B536**, 177 (2002); C.S. Fischer, R. Alkofer, H. Reinhardt, Phys. Rev. **D65** 125006 (2002); R. Alkofer, C.S. Fischer, L. Von Smekal, Acta Phys. Slov. **52** 191 (2002)
40. M.S. Bhagwat *et al.*, Phys. Rev. **C68**, 015203 (2003) 189 (1985)
41. S. Furui and H. Nakajima, Phys. Rev. **D70**, 094504 (2004)
42. J. M. Maldacena, Adv. Theor. Math. Phys. **2** 252 (1998); Int. J. Theor. Phys. **38**, 1113 (1999)
43. See for ex. J. Polchinski and M. J. Strassler, Phys. Rev. Lett **88**, 031601 (2002); JHEP **0305**, 012 (2003); S. J. Brodsky and G. F. de Teramond, Phys. Rev. Lett **94**, 201601 (2005); Phys. Rev. Lett. **96**, 201601 (2006). A. Karch, E. Katz, D. T. Son and M. A. Stephanov, Phys. Rev. **D74**, 015005 (2006)
44. JLab experiment E08027. K. Slifer, A. Camsonne and J-P. Chen spokespersons.